Role of magnetic anisotropy in spin-filter junctions

R.V. Chopdekar,[1,2*] Franklin Wong,[1,3] B.B. Nelson-Cheeseman,[1†] M. Liberati,[4] E. Arenholz,[4] Y. Suzuki[1,3]

[1] Department of Materials Science and Engineering, UC Berkeley, Berkeley, CA 94720
[2.] School of Applied and Engineering Physics, Cornell University, Ithaca, NY, 14853
[3.] Materials Science Division, Lawrence Berkeley National Laboratory, Berkeley, CA 94720
[4.] Advanced Light Source, Lawrence Berkeley National Laboratory, Berkeley, CA 94720

ABSTRACT

We have fabricated oxide based spin filter junctions in which we elucidate the role of magnetic anisotropy in the transport behavior of spin filter junctions. Until recently, spin filters have been largely comprised of polycrystalline materials where the spin filter barrier layer and one of the electrodes are ferromagnetic. While these spin filter junctions have relied on the weak magnetic coupling between one ferromagnetic electrode and a barrier layer or the insertion of a nonmagnetic insulating layer in between the spin filter barrier and electrode, we have demonstrated that by careful choice of the magnetic anisotropy of the ferromagnetic layers, we can tune the interface anisotropy and hence the junction magnetoresistance in epitaxial oxide based spin filter junctions.

† presently at Argonne National Laboratory, Argonne, IL, 60439.

INTRODUCTION

Spin polarized devices such as magnetic tunnel junctions have been recognized as potential building blocks for a new type of spin based electronics in recent years. While magnetic tunnel junctions, which are composed of two ferromagnetic electrodes sandwiching an insulating barrier, were first conceived in 1975 by Julliere,[i] it was not until the 1990s that significant junction magnetoresistance was demonstrated in magnetic tunnel junctions at room temperature[ii] and it was realized that transport through these structures is extremely sensitive to the interface scattering and spin polarized interface density of states of the electrode.[iii] Briefly, in magnetic tunnel junctions it is the relative orientation of the electrode magnetization that determines whether the junction exhibits a high or low resistance state with the junction magnetoresistance being defined as the fractional change of resistance between these two states. It was not until recently, however, that the importance of understanding the role of the barrier layer in the tunneling process was recognized in experimental and theoretical studies of magnetic tunnel junctions with MgO barriers.[iv] In these junctions, the symmetries of the propagating states in the electrodes and the evanescent states in the barrier, interface resonance states as well as the details of the chemical bonding between the atoms in the electrodes and barrier were recognized to be important factors in describing the spin transport.

Another important class of spin polarized devices is a so-called spin filter device in which one electrode and the barrier layer are ferromagnetic; the relative orientation of the magnetization in the two layers again determines whether the device is in a high or low resistance state. In such devices, the ferromagnetic barrier layer has spin filtering functionality and has often been simply described as a finite potential barrier whose height depends on the spin polarization of the carrier. However it is clear that interaction between the carriers and the barrier make spin transport more complicated. In any case, effective spin filtering can occur when the two ferromagnetic layers are magnetically decoupled so that one can obtain a significant difference in resistance between the parallel low resistance state and the anti-parallel high resistance state. This magnetic decoupling had, up until recently, only been realized in polycrystalline spin filter junctions with and without a nonmagnetic layer separating the two ferromagnetic layers.[v,vi]

Recently, however, we have realized weak magnetic coupling of adjacent epitaxial layers that has enabled us to demonstrate spin filtering behavior in epitaxial oxide junctions.[vii] These junctions are composed of one cubic perovskite structure $La_{0.7}Sr_{0.3}MnO_3$ (LSMO) electrode, a cubic spinel structure barrier layer and electrode. The weak magnetic coupling occurs at the interface of the ferromagnetic perovskite electrode and ferrimagnetic spinel barrier layer due to magnetic frustration. In these junctions, a ferrimagnetic Fe_3O_4 electrode was used as it was strongly coupled to the barrier layer and its magnetization provided a handle with which to magnetically switch the barrier layer. In order to understand the role of magnetic anisotropy and magnetic frustration in determining the spin filtering behavior, detailed studies of the isostructural and non-isostructural interfaces and correlation with magnetotransport are necessary.

In this paper, we have fabricated LSMO/ chromite/ Fe_3O_4 junctions where the chromite barrier layer is either $CoCr_2O_4$ (CCO) or $MnCr_2O_4$ (MCO)- both of which are isostructural with Fe_3O_4. Although both chromite compounds form a normal spinel with all Cr^{3+} ions in the octahedral sites, the magnetic anisotropy of the two compounds are opposite in sign and thus give rise to junction magnetoresistance values over an order of magnitude higher in CCO junctions compared to MCO junctions. Detailed studies of chemical and magnetic structure at the interfaces in both types of junctions indicate that abrupt changes in magnetic anisotropy across the non-isostructural interface is the cause of the significant suppression of JMR in MCO junctions. Therefore magnetic anisotropy provides means by which we can tune junction behavior.

EXPERIMENT

Both LSMO and Fe_3O_4 have been shown to be highly spin polarized and therefore are good candidates for magnetic tunnel junctions.[viii,ix,x] The lattice of LSMO can be described in terms of a pseudocubic unit cell with 3.87Å on a side while Fe_3O_4 forms a cubic spinel with 8.396Å on a side. The barrier layer has been chosen to be either CCO or MCO both of which are ferrimagnetic below and paramagnetic above their respective T_c's of 95K and 45K. Both CCO and MCO have lattice parameters of 8.333 and 8.437Å respectively and are well matched to the Fe_3O_4.

The trilayers of $La_{0.7}Sr_{0.3}MnO_3$(LSMO)/$CoCr_2O_4$/ Fe_3O_4 and $La_{0.7}Sr_{0.3}MnO_3$/Mn Cr_2O_4/ Fe_3O_4 were synthesized by pulsed laser deposition on (110) oriented $SrTiO_3$ (STO) substrates supplied by Crystec GmbH. Commercial sintered powder targets of stoichiometric single-phase oxides were used for ablation at an energy density of 1-1.5 J/cm^2. Deposition parameters for the layers are as follows: LSMO in 320 mTorr of O_2 at 700°C; Fe_3O_4 in a vacuum of better than $4x10^{-6}$ Torr at 450°C; $MnCr_2O_4$ and $CoCr_2O_4$ in 25 mTorr of O_2 at 600°C. Thicknesses of the LSMO and Fe_3O_4 electrodes were approximately 30-50nm while the chromite barriers were 2-4nm thick. Following thin film growth, one half of twin samples were characterized for coercive fields and morphology while the other half were fabricated into junctions between 4 x 4μm^2-40 x 40μm^2 in area. The junctions were fabricated by conventional photolithography and Ar ion mill. In addition, bilayer samples of chromite/LSMO/(110)STO and Fe_3O_4/chromite/(110)STO were synthesized in order to probe the non-isostructural and isostructural interfaces respectively using element specific X-ray absorption spectroscopy (XAS) and X-ray magnetic circular dichroism (XMCD). The surface sensitive nature of these probes required us to make these bilayers with a top layer thickness of 2nm to ensure that we were able to probe the two types of interfaces.

The structure of our films was characterized by X-ray diffraction on a Philips Analytical X'pert MRD diffractometer and by cross sectional transmission electron microscopy (TEM) using the electron microscope at the National Center for Electron Microscopy in Lawrence Berkeley National Laboratory. Bulk magnetization measurements were performed in a Quantum Design MPMS 5XL magnetometer and resistivity measurements were performed in a modified Quantum Design Physical Property Measurement System. XAS and XMCD experiments in total electron yield (TEY) mode were performed at beamlines 4.0.2 and 6.3.1 of the Advanced Light Source (ALS) at Lawrence Berkeley National Laboratory.

Spectroscopy experiments were performed with the sample surface normal 60◦ inclined from the x-ray beam from 25 K-325 K in fields of up to 0.8 T.

STRUCTURE

Structural characterization in the form of four-circle X-ray diffraction and transmission electron microscopy (TEM) were performed. Phase-contrast TEM imaging shows that chromite-ferrite interfaces show excellent registry with minimal defects (Figure 1). In addition, good registry between perovskite and chromite film layers can be obtained with little disorder at the non-isostructural interface. Fourier transforms of the lower and upper sections show that the LSMO and chromite layers are both oriented with the (110) direction out of plane. During high temperature growth, the interdiffusion of chemical species cannot be avoided. We have demonstrated in a previous study that nanoscale cation migration does occur at isostructural interfaces and that it induces room temperature ferromagnetism in the chromite.[xi,xii] In order to correlate the structure with magnetism, we have used XAS and XMCD to probe the chemical and magnetic structure in an element specific manner at both interfaces.

MAGNETISM

An understanding of the magnetism in the LSMO, Fe3O4 and chromite layers as well as at their interfaces is crucial in determining the dominant mechanism in the transport of junctions based on these materials. Through a combination of SQUID magnetometry that probes the bulk film properties and XMCD, we have developed a complete picture of the magnetism in these junction trilayers.

Bulk magnetization measurements of the trilayers reveal a magnetically easy axis along the in-plane [001] direction and a hard axis perpendicular in the [1-10] direction as shown in Figure 2a and b for both types of junctions. Despite small differences in the plots, we observe along the [001] direction, distinct parallel and anti-parallel electrode magnetization states. Because the magnetic signal from the chromite barrier layer is so small, we cannot probe the chromite magnetism via bulk SQUID magnetization measurements. In order to study the magnetism of the chromite layer and at its two interfaces, we used XMCD on the two bilayer samples described above.

Let us first consider the isostructural chromite/Fe_3O_4 interfaces. Magnetic characterization using XMCD provides us with magnetic moment versus magnetic field in an element specific manner, thus enabling us to probe the coupling among magnetic species across the interfaces. At low temperatures (below the chromite T_c) one may expect that the ferrimagnetic chromite layers strongly exchange couple to the Fe_3O_4, but it is less clear as to the nature of the coupling above the chromite T_c. Room temperature element-specific hysteresis loops at the Fe L_3 edge along the [001] and [1-10] directions are shown in the solid lines of Figure 3. They reveal that the presence of Co and Mn have marked effect on the anisotropy and coercivity of the Fe_3O_4 cap layer, even though it is the Cr that interdiffuses more strongly into the Fe_3O_4 from the EELS data in our previous work.[12] The CCO bilayer shows an increase of the Fe_3O_4 coercive field to approximately 1000 Oe along

the [001] direction, and the sample could not be saturated even in 2000 Oe along the [1-10] direction. On the other hand, the MCO coercive field was approximately 500 Oe but the anisotropy of the Fe_3O_4 cap layer reversed so that the easy axis is along the [1-10] in-plane direction. Comparison to cobalt and manganese ferrites show that the coercivity and anisotropy behavior matches the behavior in these samples, and thus the Cr at the interface does not have a large influence on the room-temperature interface magnetism. Coincident loops of Cr, Co, and Fe and Cr, Mn and Fe confirm that the interface chromite layer is coupled strongly to the Fe_3O_4 layer even at room temperature.

At the nonisostructural interface, we find significantly less magnetic coupling between the LSMO and chromite layers. Previously, we and other groups have found that the growth of a spinel structure material on top of a cubic perovskite with half the unit cell can give rise to anti-phase boundaries and misfit dislocations.[xiii,xiv] These defects, along with the ferromagnetic LSMO and ferrimagnetic chromite lattices, give rise to magnetic frustration. In order to probe the magnetism of such an interface in more detail, the (110) LSMO/MCO interface was explored in an analogous manner to the Fe_3O_4/MCO interface. At room temperature and at 100 K, the XMCD lineshapes at the Mn $L_{2,3}$ edge were identical to the XMCD lineshapes of the octahedral Mn^{3+} and Mn^{4+} in a LSMO/STO sample even though the XAS lineshape was dominated by the tetrahedral Mn^{2+} in the MCO cap layer (Figure 3 (a)) in contrast to the octahedral Mn^{3+} and Mn^{4+} LSMO. Below the MCO T_c, the XMCD lineshape becomes dominated by the magnetism in the MCO cap layer. Element-specific hysteresis loops at the Mn edge sample Mn in both layers, but Cr edge loops sample only the magnetism in the MCO cap layer. By tuning the photon energy to match the maximum dichroism for the MCO layer (line A = 640.0 eV) or near the maximum dichroism for LSMO but close to zero dichroism for a single MCO layer (line B = 642.4 eV), we find that the hysteresis loops can show the field dependence of Mn in either of the MCO or LSMO layers. Figure 3 (b) indicates that the (110)LSMO retains its uniaxial anisotropy with the magnetically hard direction along the in-plane [1-10] direction. The reduction in magnitude between 15 K and 45 K is an artifact due to a small positive contribution of the MCO dichroism lineshape reducing the LSMO dichroism at 642.4 eV. For the 15 K and 45 K cases, above the anisotropy field of approximately 3500 Oe the LSMO signal seems to decrease in magnitude. Comparison to Mn hysteresis loops taken at 640.0 eV as well as Cr hysteresis loops (Figure 3 (c) and (d)) show that the MCO layer is frustrated by the LSMO underlayer and does not saturate even out to 8000 Oe, despite the [1-10] direction being the easy axis for (110)MCO single layers. Thus the orthogonal easy axes for (110) LSMO and (110)MCO frustrate each other resulting in a lack of saturation for the bilayer as a whole.

Similar results may be obtained from the equivalent Mn and Cr loops measured along the [001] direction (Figure 3 (e) and (f)). At 100K the Mn in the LSMO layer saturates in a field of less than 200 Oe and there is no magnetic signal from the Cr in the MCO. When the temperature is reduced to below the T_c of the MCO in bulk, the MCO magnetization prevents saturation of the LSMO up to fields of 1000 Oe, with identical non-saturating behavior seen in the Cr and Mn edge hysteresis loops. This magnetic frustration has implications for magnetotransport.

In contrast to the magnetic frustration at the LSMO/MCO interface, the LSMO/CCO interface reveals the magnetically easy axis in both (110)LSMO and (110)CCO to be along the in-plane [001] direction and a hard axis along the in-plane [00-1] direction perpendicular to the easy direction. These results are consistent with those of single layer (110) epitaxial thin films of these materials grown on (110) STO substrates.[12] Detailed XMCD investigations reveal that there is strong coupling at the Fe_3O_4/CCO interface and very weak magnetic coupling at the LSMO/CCO interface. XMCD-based hysteresis loops of Mn and Cr show no evidence of any magnetic frustration at the LSMO/CCO interface. The coincidence of the magnetically easy axes in the perovskite and spinel layer is manifest in the magnetotransport measurements.

JUNCTION TRANSPORT BEHAVIOR

When these two types of interfaces are incorporated into a single magnetic junction, we observe markedly different magnetotransport behavior for the two types of junctions. High field junction magnetoresistance (JMR) values on the order of -30% were achieved by incorporating a CCO barrier layer with LSMO and Fe_3O_4 electrodes and further studies have confirmed that similar barrier layers such as $FeGa_2O_4$, Mg_2TiO_4, and $NiMn_2O_4$ can produce similarly large JMR values.[xv] The relatively high JMR values compared to other epitaxial oxide based junctions is due in part to the use of (110) oriented LSMO in which the surface magnetization is more robust than the (001) orientation.[xvi] Despite the substantial JMR that we observe in CCO junctions, we found almost an order of magnitude smaller JMR in corresponding junctions with MCO barrier layers. A detailed investigation of the temperature and bias dependence of the JMR provides us insight into the transport mechanism and the source of this contrasting behavior.

The voltage and temperature dependence of the JMR can be summarized in a two-dimensional plot as shown in figure 4 for a Fe_3O_4/2nmCCO/LSMO junction. A quick look at the plot indicates that there are three temperature regimes; : T=0-70 K, T=70-175 K, and T=175-300 K. In the lowest temperature region, the JMR decreases with decreasing temperature in contrast to the expected increase of LSMO spin polarization with decreasing temperature. In this temperature regime, the Fe_3O_4 electrode resistance is large due to the Verwey metal-insulator transition, and the JMR is obscured by the Fe_3O_4 resistance.

In the intermediate temperature region, the bias dependence of the JMR is asymmetric and the JMR increases with decreasing temperature. An isothermal cutline (Figure 5, right panel) illustrates this asymmetry quite clearly for a 4 nm CCO barrier. In this temperature region, the spin polarization of the electrodes is large at low temperatures, but the asymmetric structure of the barrier/electrode interfaces produces an asymmetric conduction barrier. There have been numerous studies of magnetic tunnel junctions where asymmetries in the JMR bias dependence have been attributed to the two different interface density of states at the two electrode-barrier interfaces.[xvii] In our case, it is not surprising that the isostructural and non-isostructural interfaces give rise to distinctly different density of states. We also observe a zero bias anomaly whose origin we attribute to the opening up of a charge gap in the Fe_3O_4 below the Verwey transition. The JMR minimum at 50-100mV is consistent with observed charge gaps in Fe_3O_4.[xviii]

In the highest temperature region, the magnitude of JMR is negligible and has little bias dependence. One might wonder why the spin polarization seems to decrease so much above 175 K if the Fe_3O_4 T_c is 858K and the LSMO T_c is 360 K . Our previous study on the temperature dependence of the magnetic coupling at the Fe_3O_4/CCO interface indicates that the magnetization of the Fe, Cr and Co sublattices decrease substantially between T=150-200K. Thus it is expected that the spin-filtering efficiency for the exchange-coupled chromite-Fe_3O_4 bilayer also decreases substantially in this temperature region. Additionally, temperature-dependent measurements with LSMO electrodes and nonmagnetic barrier layers have shown that the interface spin polarization is suppressed almost as much as the surface spin polarization.[xix] Suppression at both interfaces leads to a vanishingly small JMR at room temperature.

Similar JMR measurements on MCO junctions showed significantly suppressed maximum JMR values, on the order of ~-1%, compared with corresponding CCO junctions. In order to explain this suppression of JMR, we probed the bulk magnetic response of the trilayer as a function of magnetic field direction. Figure 6 shows that for fields applied along the [001] direction, both junctions exhibit well defined parallel and anti-parallel magnetic states. In fact, it is the MCO junction that has sharper magnetic transitions for both the LSMO and Fe_3O_4 electrodes. Magnetic signal from the barrier is too small to be detected in such a bulk magnetization curve. Therefore the suppressed JMR must be due to the differences in interface magnetic anisotropy at the LSMO/chromite interfaces.

If indeed the interface magnetic anisotropy is the cause of the JMR suppression, the JMR in MCO and CCO junctions as a function of the applied magnetic field direction should be distinctly different. The angular dependence of the JMR is shown in Figures 6 and 7 for CCO and MCO junctions respectively. For each plot, the temperature is fixed at 130K and the sample is saturated at 30kOe for each in-plane angle measured. The JMR values are normalized to the zero field resistance values. The maximum JMR values for both junctions are found to be along the [001] direction while the minimum values are along the [1-10] directions. However at this temperature, the maximum JMR value for the CCO junction in Figure 6 is -6% which is an order of magnitude higher than that for the MCO junction of -0.7%. In addition, there appear additional JMR extrema along the [1-11] directions in the MCO junctions. The stabilization of relatively high JMR along the [1-11] directions is most likely due to a modification of the crystal anisotropy constants (K_n) at the interface due to the addition of Mn into Fe_3O_4. Therefore despite well defined parallel and anti-parallel states in the LSMO and Fe_3O_4 electrodes for both types of chromite junctions along the [001] direction, it is the stabilization of CCO moments at both interfaces along the [001] direction that gives rise to high JMR. The stabilization of MCO moments along the [1-10] direction gives rise to magnetic frustration and reduced JMR.

From these magnetotransport results, it is clear that the interface plays an important role in determining the spin filtering efficiency of these junctions. What is interesting to note is that strong magnetic anisotropy is induced in the chromite barrier layer even above its nominal bulk magnetic transition temperature. We had already observed proximity induced ferromagnetism in $CoCr_2O_4$ / Fe_3O_4 bilayers in the past.[12] However our present

studies makes it clear that it is not the Fe_3O_4 layer that dictates the magnetic anisotropy of the chromite layer but rather the chromite/ferrite interface itself. It is this strong interface magnetic anisotropy and its coincidence (for CCO) and frustration (for MCO) with the LSMO magnetic anisotropy that dictates the transport.

CONCLUSION

In summary, we have fabricated oxide-based spin filter junctions in which we have shown that the junction transport is dictated by the magnetic anisotropy at the interface between the spin filter barrier layer and each electrode. In both types of chromite junctions, the Fe_3O_4 is strongly magnetically coupled to the chromite barrier layer and is only weakly magnetically coupled to the LSMO electrode. The coincidence of the magnetically easy axes in the chromite and LSMO layers in the CCO junctions enables the establishment of distinct parallel and antiparallel magnetization states, thus giving rise to significant junction magnetoresistance. In MCO junctions, the easy axes of the MCO and LSMO layers are perpendicular to one another, thus giving rise to magnetic frustration and suppressed junction magnetoresistance. Therefore it is clear that magnetic anisotropy at the electrode/barrier interface plays an important role in determining spin transport in this class of devices.

ACKNOWLEDGMENT

The authors would like to thank Prof. Angelica Stacy for the use of her θ-2θ diffractometer and Dr. Kin Man Yu from the Lawrence Berkeley National Laboratory Materials Science Division for taking RBS spectra. This research is supported by the National Science Foundation (DMR 0604277). FW, the Advanced Light Source and the National Center for Electron Microscopy are supported by the Director, Office of Science, Office of Basic Energy Sciences, of the U.S. Department of Energy under Contract No. DE-AC02-05CH11231.

FIGURES

Figure 1 – TEM micrograph of the interface between perovskite structure (110) LSMO and a spinel chromite multilayer.

Figure 2. – Major magnetic hysteresis loops for unpatterned trilayers with CCO barrier (left) or MCO barrier (right).

Figure 3. – Room temperature element-specific hysteresis loops for an Fe_3O_4/CCO/STO sample measured with magnetic field along the (a) [001] or (b) [1-10] in-plane direction, and an Fe_3O_4/MCO/STO sample along the (c) [001] or (d) [1-10] in-plane direction

Figure 4 – (a) Mn $L_{2,3}$ XAS and XMCD lineshapes of an LSMO/MCO capped sample as a function of temperature, with (b)-(f) as element-specific hysteresis loops of Mn or Cr taken either along the [001] or [1-10] in-plane direction as indicated. Line A denotes E=640.0 eV, and line B denotes E=642.4 eV.

Figure 5. – Junction magnetoresistance map as a function of bias and temperature for a device with a 4 nm CCO barrier layer, and isothermal cutline across map (right) to show non-monotonic bias dependence.

Figure 6. – Junction magnetoresistance map as a function of magnetic field and azimuthal angle for a 2 nm CCO based junction.

Figure 7. – Junction magnetoresistance map as a function of magnetic field and azimuthal angle for a 2 nm MCO based junction.

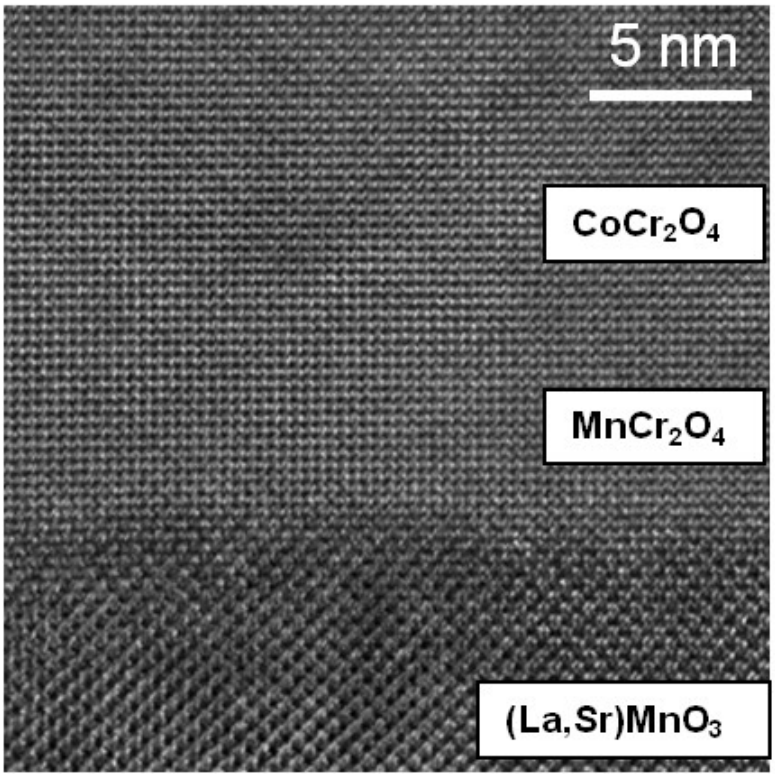

Figure 1.

Chopdekar et al.

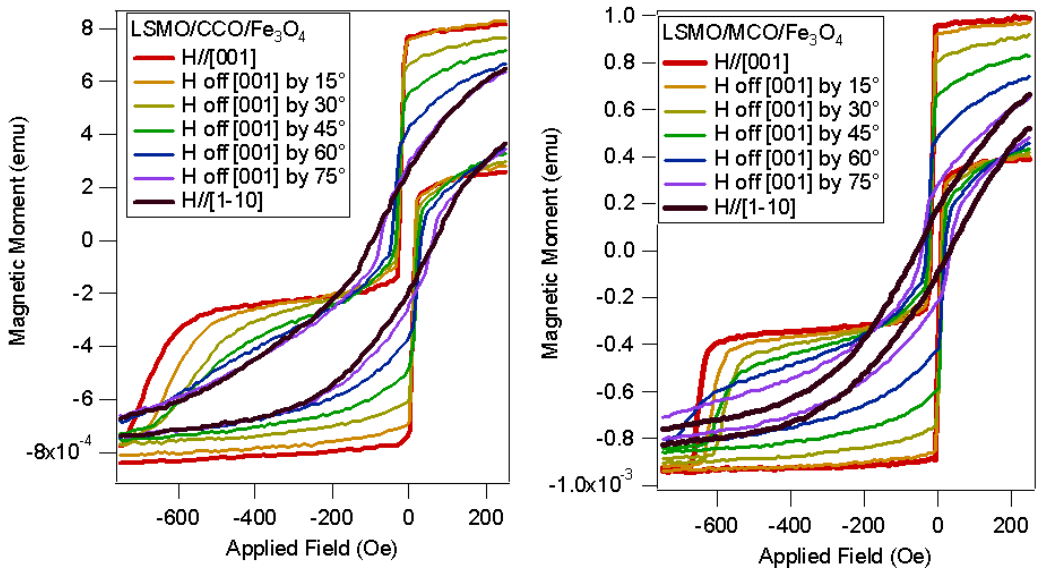

Figure 2.
Chopdekar et al.

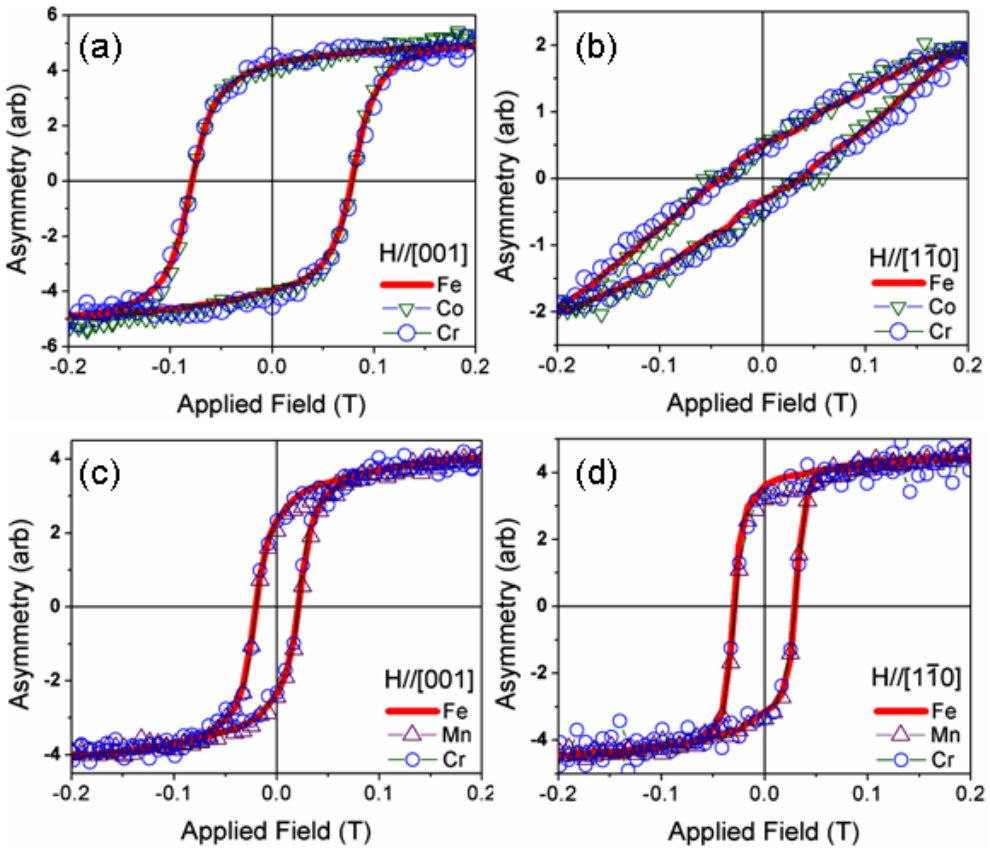

Figure 3.
Chopdekar et al.

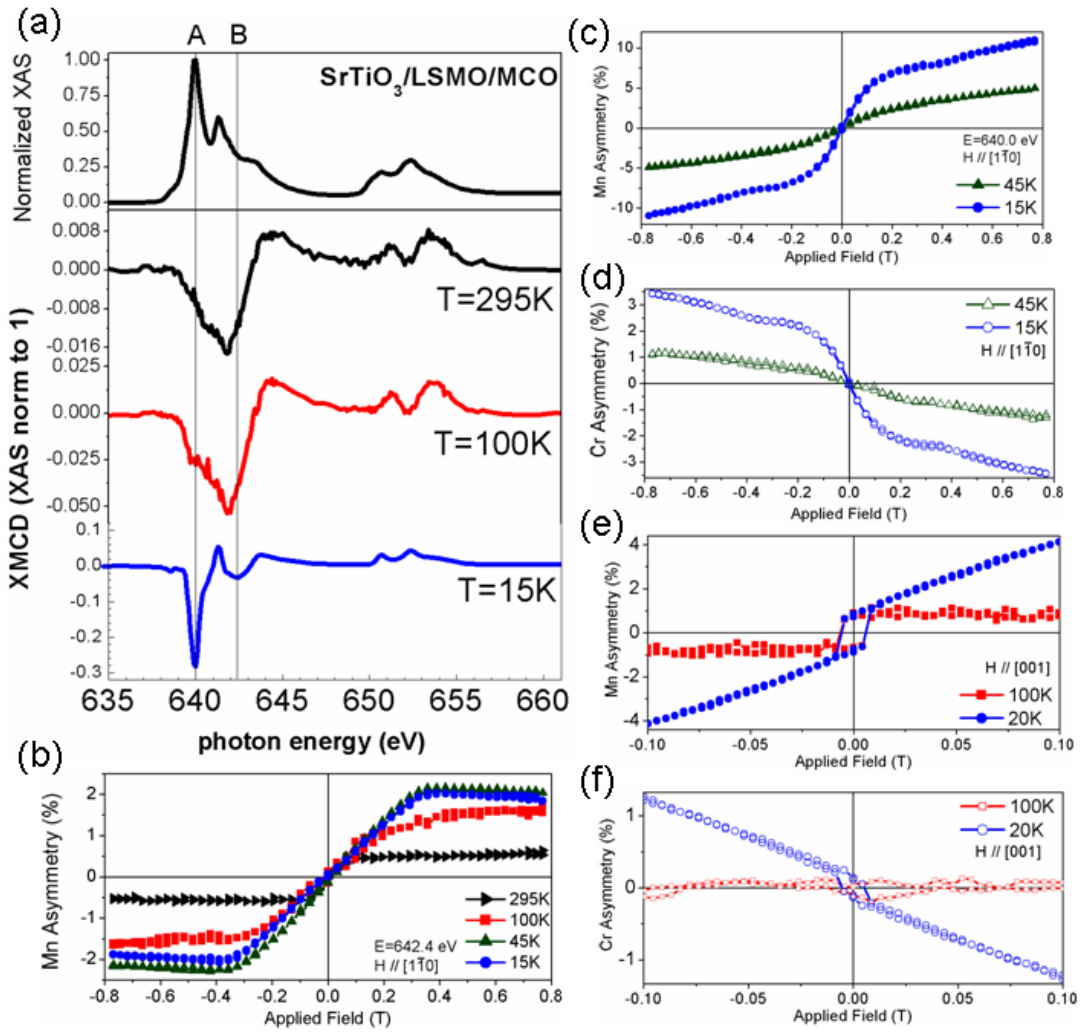

Figure 4.
Chopdekar et al.

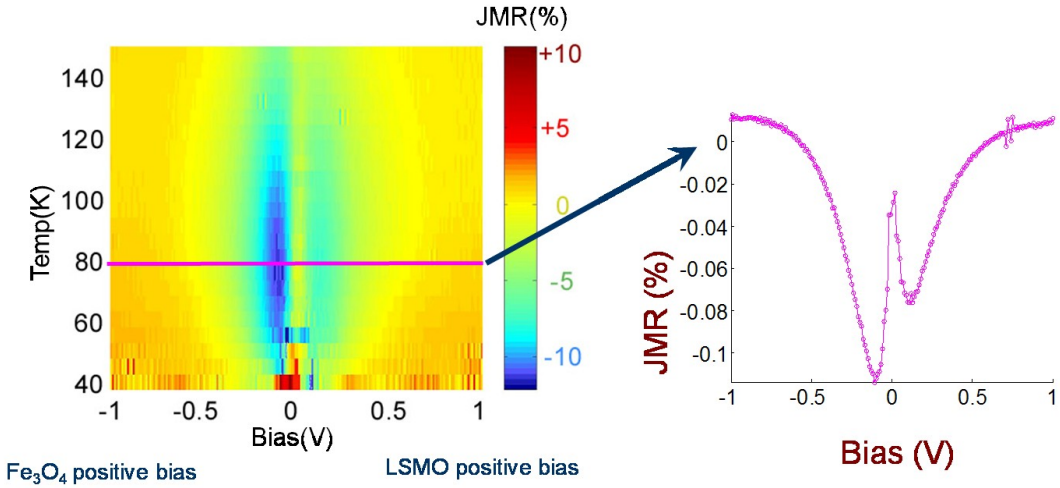

Figure 5.
Chopdekar et al.

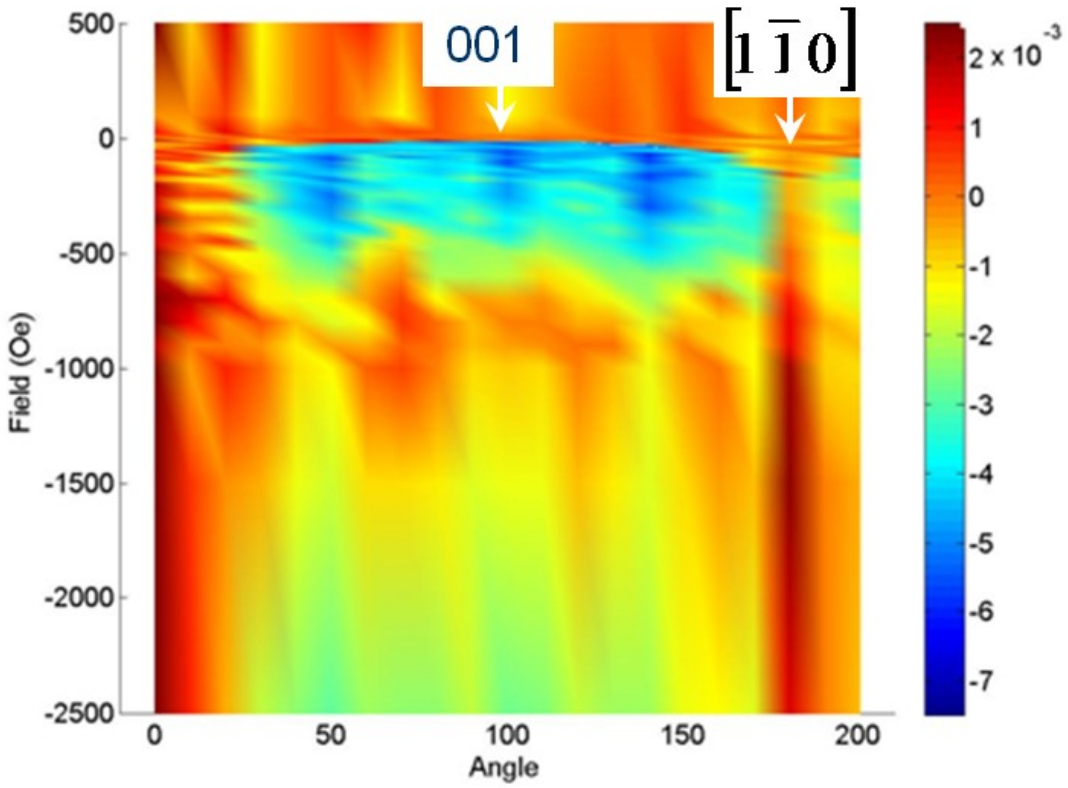

Figure 6.
Chopdekar et al.

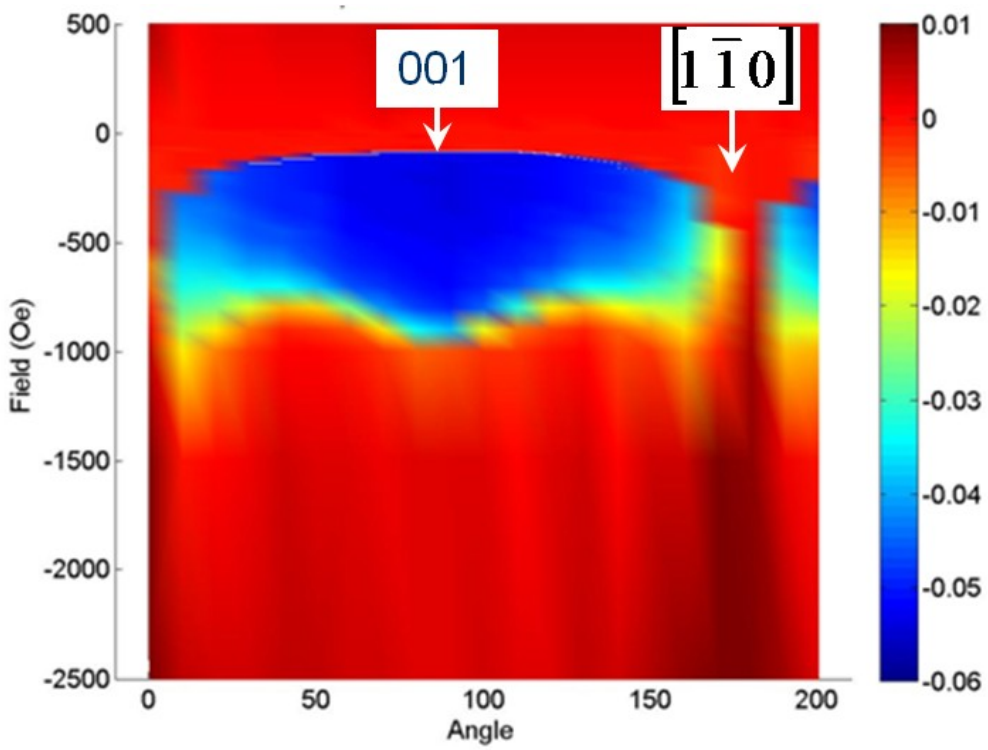

Figure 7.
Chopdekar et al.

REFERENCES

[i] M.Julliere, Phys. Lett. 54A, 225 (1975).

[ii] J.S. Moodera, L.R. Kinder, T.M. Wong, and R. Meservey, Phys. Rev. Lett. 74, 3273 (1995).

[iii] G.T. Woods, R.J. Soulen,Jr., I.I. Mazin, B. Nadgorny, M.S. Osofsky, J. Sanders, H. Srikanth, W.F. Egelhoff, R. Datla, Phys. Rev. B. 70, 054416 (2004).

[iv] W.H. Butler, X.-G. Zhang, T.C. Schulthess, J.M. MacLaren, Phys. Rev. B 63, 054416 (2001).

[v] P. LeClair, J. K. Ha, H. J. M. Swagten, J. T. Kohlhepp, C. H. van de Vin, and W. J. M. de Jonge, Appl. Phys. Lett. **80**, 625 (2002).

[vi] T. Nagahama, T.S. Santos, J.S. Moodera, Phys. Rev. Lett. **99,** 016602 (2007).

[vii] B.B. Nelson-Cheeseman, R.V. Chopdekar, L.M.B. Alldredge, J.S. Bettinger, E. Arenholz, Y. Suzuki, Phys. Rev. B **76** R220410 (2007*)*

[viii] J.S. Noh, T.K. Nath, C.B. Eom, J.Z. Sun, W. Tian, X.Q. Pan, Appl. Phys. Lett. **79** 233 (2001).

[ix] Yu. S. Dedkov, U. Rudiger, and G. Guntherodt, Phys. Rev. B **65**, 064417 (2002).

[x] D. J. Huang *et al.*, J. Magn. Magn. Mater. **239**, 261 (2002).

[xi] Rajesh V. Chopdekar, Guohan Hu, Alexandra C. Ford, Yuri Suzuki, IEEE Trans. Mag. **40** 2302 (2004).

[xii] R.V.Chopdekar, M. Liberati, Y. Takamura, L. Fitting Kourkoutis, J. S. Bettinger, B.B. Nelson-Cheeseman, E. Arenholz, A. Doran, A. Scholl, D. A. Muller, and Y. Suzuki, unpublished (2010).

[xiii] G. Hu, V.G. Harris, Y. Suzuki, IEEE Trans. Mag. **37** 2347 (2001).

[xiv] D. T. Margulies, F. T. Parker, M. L. Rudee, F. E. Spada, J. N. Chapman, P. R. Aitchison, and A. E. Berkowitz, Phys. Rev. Lett. **79**, 5162 (1997).

[xv] L.M.B. Alldredge, R.V. Chopdekar, B.B. Nelson-Cheeseman, Y. Suzuki, Appl. Phys. Lett. **89** 182504 (2006).

[xvi] Rajesh V. Chopdekar, Elke Arenholz, Yuri Suzuki, Phys. Rev. B **79** 104417 (2009).

[xvii] J.S. Moodera and G. Mathon, J. Magn. Mag. Mater. **200** 248 (1999).

[xviii] S. K. Park, T. Ishikawa, and Y. Tokura, Phys. Rev. **58** 3717 (1998).

[xix] J. H. Park E. Vescovo, H.-J. Kim, C. Kwon, R. Ramesh, and T. Venkatesan, Phys. Rev. Lett. **81**, 1953 (1998).